

A new cyclic RGD peptide dimer for integrin $\alpha_v\beta_3$ imaging

H. MA¹, P. HAO¹, L. ZHANG², C. MA³, P. YAN¹, R.-F. WANG¹, C.-L. ZHANG¹

¹Department of Nuclear Medicine, Peking University First Hospital, Beijing, China

²Department of Nuclear Medicine, Beijing Millennium Monument Hospital Affiliated to Capital Medical University, Beijing, China

³Department of Nuclear Medicine, Zhongshan Hospital affiliated to Xiamen University, Xiamen, China

Abstract. – OBJECTIVE: To design a new Arg-Gly-Asp (RGD) peptide that can specifically bind integrin $\alpha_v\beta_3$ and evaluate the possibility of using ¹³¹I-labeled peptide for imaging $\alpha_v\beta_3$ -positive tumors.

MATERIALS AND METHODS: The structure of the RGD monomer was selected using V-life software. Based on the RGD monomer, a dimer of cyclic RGD [c(RGD)₂] linked by Tyr-(D)Ser-Lys-(D)Ser-Ser with a Gly-Gly-(D)Ala-Gly side chain on the lysine residue was synthesized. ¹³¹I-c(RGD)₂ was synthesized using the chloramine-T (ChT) method, and the octanol-water partition coefficient was experimentally measured. To evaluate its binding affinity and selectivity, its equilibrium dissociation constant (Kd) with U87 MG glioma cells was measured *in vitro*, while whole body imaging and biodistribution were assessed *in vivo* in mice bearing U87 MG xenografts.

RESULTS: The optimal structure of the monomer was cyclic [-Cys-Arg-Gly-Asp-(D)Ser-Cys-]. The ¹³¹I-c(RGD)₂ molecule exhibited good stability and was highly hydrophilic. The Kd value was $(3.87 \pm 0.05) \times 10^{-9}$ M, suggesting a high $\alpha_v\beta_3$ -binding affinity and specificity. The tumors were clearly visualized at 3 and 6 h post-injection. Biodistribution data of the ¹³¹I-c(RGD)₂ molecule showed rapid clearance from the blood and predominant accumulation in the tumor and kidney. The tumor-to-normal tissue (T/NT) ratio increased over time. At 24 h post-injection, the tumor-to-liver, tumor-to-muscle, and tumor-to-blood ratios were 4.92, 4.29, and 5.00, respectively.

CONCLUSIONS: These results suggest that the ¹³¹I-c(RGD)₂ molecule may serve as a promising tracer for the detection of $\alpha_v\beta_3$ -positive tumors.

Key Words:

Radionuclide labeling, Radionuclide imaging, Integrin $\alpha_v\beta_3$, RGD peptides.

Introduction

Integrins are a well-known family of cell adhesion molecules that play an important role in tumor angiogenesis, which is necessary for both tumor growth and metastasis¹. Integrins are heterodimeric glycoproteins composed of an α - and a β -subunit. To date, 25 combinations of the 19 α - and 8 β -subunits have been identified². Among them, the integrin $\alpha_v\beta_3$ is likely the most strongly involved in the regulation of angiogenesis and is drawing increasing attention³. The expression of integrin $\alpha_v\beta_3$ is up-regulated in the tumor vasculature and on a variety of solid tumor surfaces, but it is low in both resting endothelial cells and most normal organ systems^{4,7}. Integrin $\alpha_v\beta_3$ can regulate cell proliferation, survival, differentiation, migration, and mechanotransduction through bidirectional signal transduction^{8,9}. It is vital for the interaction of endothelial cells with extracellular matrix proteins (e.g., vitronectin, fibronectin, and collagen) during angiogenesis, which occurs via their Arg-Gly-Asp (RGD) tripeptide sequence¹⁰. Integrin $\alpha_v\beta_3$ is not only capable of producing independent signals, but it also exhibits cross-talk with signals generated by soluble factors. For example, vascular endothelial growth factor receptor-2 and integrin $\alpha_v\beta_3$ jointly regulate vessel formation¹¹⁻¹³. Recently, integrin $\alpha_v\beta_3$ has been shown to be an efficient molecular target for therapeutic drugs and angiogenesis imaging agents¹⁴.

The RGD sequence is currently the basic module for many radiotracers that have been designed to specifically bind to integrin $\alpha_v\beta_3$. The first radiotracer used to image integrin $\alpha_v\beta_3$ was introduced in 1999¹⁰. Currently, a variety of RGD derivatives have been described, but only a small set has entered clinical trials. [¹⁸F]Galacto-RGD has been used in clinical studies and ex-

hibits a predominantly rapid renal elimination and a low radiation burden for patients. Nevertheless, the low tumor-to-background ratio limits its wide clinical application¹⁵. Thus, one important direction for molecular nuclear medicine involving integrin $\alpha_v\beta_3$ receptor research is to improve $\alpha_v\beta_3$ targeting and reduce the compound concentration in non-cancerous organs.

Recently, the concept of polyvalency has been used to enhance the binding affinity of multimeric RGD peptides. The binding affinity and tumor incept of RGD derivatives follow the sequence octamer > tetramer > dimer > monomer¹⁴. However, with increasing peptide multiplicity, the uptake of radiolabeled multimeric RGD derivatives in non-targeted organs also markedly increases¹⁶. In addition, the cost of RGD tetramers and RGD octamers is prohibitively high for the development of $\alpha_v\beta_3$ -targeted derivatives¹⁷. The binding affinity of cyclic RGD peptide tetramers to $\alpha_v\beta_3$ is bivalent, although they have four identical RGD motifs^{18,19}.

Due to the drawbacks of the multimeric RGD peptides mentioned above, the use of dimeric scaffolds is more favorable. Cyclization of RGD peptides via linkers, such as double disulfide bonds, often leads to a higher receptor binding affinity and selectivity²⁰. The RGD peptides that include two disulfide bonds are at least 20-fold more potent inhibitors of integrin $\alpha_v\beta_3$ -mediated cell attachment than those with a single disulfide bond, and they are 200-fold more potent than commonly used linear RGD peptides²¹.

In this study, a novel cyclic RGD peptide [c(RGD)₂] with double disulfide bonds was synthesized, and the characteristics of ¹³¹I-labeled c(RGD)₂ were evaluated. The probe was applied to a subcutaneous U87 MG xenograft (human glioblastoma) model with high integrin $\alpha_v\beta_3$ expression⁶. Our aim was to assess the feasibility of using ¹³¹I-c(RGD)₂ as a noninvasive tumor-imaging agent.

Materials and Methods

Cell Culture and Animal Model

The U87 MG glioma cells were maintained in Dulbecco's Modified Eagle Medium (DMEM, high glucose) supplemented with 10% fetal bovine serum (Gibco, Carlsbad, CA, USA). The cells were cultured at 37°C in a humidified 5% CO₂ atmosphere and routinely passaged three to four times per week.

All animal experiments were approved by the Peking University Animal Studies Committee in accordance with the Guidelines for the Care and Use of Research Animals (Peking University, Peking, China). BALB/c nude mice from the same colony weighing 18 ± 2 g were obtained from the Department of Laboratory Animal Science of Peking University First Hospital. A 100- μ L cell suspension (1×10^7 U87 MG cells/animal) was subcutaneously inoculated into the right upper limbs of the mice. When the tumor diameter was greater than 0.8-1.0 cm, *in vivo* biodistribution and imaging analyses were performed. To block the concentration of radiotracers in the thyroid, the mice were administered 0.5% sodium iodine in their drinking water 3 days before the experiments.

Design of c(RGD)₂

The cRGD molecule library was built using the V-life software for a computer-aided drug design (CADD) system, and the cRGD peptide structure with the lowest score was identified using the DOCK procedure. The Tyr-(D)Ser-Lys-(D)Ser-Ser sequence was designed to conjugate the two cyclic RGD moieties, and a side chain -Gly-Gly-(D)Ala-Gly was linked to the lysine residue. The product was synthesized by GL Biochem Ltd. (Shanghai, China).

Radiosynthesis

The chloramine-T (CH-T) method was used for ¹³¹I-labeling of c(RGD)₂. The c(RGD)₂ (50 μ g) was diluted in 100 μ L of 0.5 M phosphate buffer (pH 7.4), and 10 μ L of ¹³¹I_{Na} (74 MBq) was then added. Fresh CH-T (9 μ L, 10 μ g/ μ L) was subsequently added to the solution. The mixture was gently shaken at room temperature for 2 min and then immediately isolated and purified by gel filtration on a Sephadex G-10 column (0.7 × 10 cm) with 0.05 M phosphate buffer (pH = 7.4) as the eluate.

As a quality control for the radiolabeled c(RGD)₂, paper chromatography on Xinhua filter paper (Hangzhou Xinhua Paper Industry Co., Ltd, China) was performed to assess the labeling efficiency and radiochemical purity. The mobile phase solution was butanol-alcohol-ammonia (5:2:1, v/v/v).

In vitro Stability

A sample of ¹³¹I-c(RGD)₂ with a concentration of 0.01 μ g/ μ L was incubated in 0.9% saline at 4°C and in fresh human serum at 37°C. Paper chromatography was performed at different time intervals to assess stability.

Octanol-Water Partition Coefficient

To determine the lipophilicity of ^{131}I -c(RGD)₂, 10 μL of column-purified ^{131}I -c(RGD)₂ was diluted in 1 mL of saline and 1 mL of octanol, and the resulting biphasic system was blended vigorously for 15 min and gently for another 10 min. The two phases were separated by vortexing (3 min, 10000 r/min), and 100- μL aliquots were removed from each phase for radioactive counting. The partition coefficient was expressed as the ratio of radioactive counts in the octanol phase to the radioactive counts in the saline phase, and $\log p$ values were calculated. The experiment was repeated 3 times.

Cell Integrin Receptor-Binding Assay

The *in vitro* integrin binding affinity of the c(RGD)₂ was assessed via displacement cell-binding assays using ^{125}I -c(RGD)₂ as the integrin-specific radioligand. The c(RGD)₂ was conjugated with ^{125}I using the Iodogen method. The U87 MG cells were scraped and diluted to a concentration of 5×10^6 /mL in the binding buffer (0.5 M Tris, pH = 7.2; 150 mM NaCl; 2 mM CaCl₂; 1 mM MgCl₂; 1 mM MnCl₂; and 1% bovine serum albumin). A cell suspension of 100 μL was placed in an Eppendorf tube and incubated with 100 μL ^{125}I -c(RGD)₂ (2×10^5 cpm) in the presence of increasing concentrations of c(RGD)₂ (0-10 nM). The total incubation volume was maintained at 300 μL . After incubation at room temperature for 2 h and centrifugation at 10000 rpm for 30 sec, the tubes were washed twice with cold binding buffer. The deposition was collected, and radioactive counts were measured using a \square -well counter (Beijing Nuclear Instrument Factory, Peking, China). The K_d values were assessed by nonlinear regression using SPSS 17.0 (SPSS Inc., Chicago, IL, USA).

SPECT Imaging

In the SPECT imaging studies, 3 mice with U87 MG tumor xenografts were injected intra-

venously with ^{131}I -c(RGD)₂ (3.7 MBq in 0.1 mL/mouse). A whole body imaging analysis was performed at 3 and 6 h after injection at the Department of Nuclear Medicine, Peking University First Hospital, using SPECT (General Electric Company, Fairfield, CT, USA). Planar images were acquired at 100,000 counts with a zoom factor of 1.0 and were digitally stored in a 256 \times 256 matrix.

Biodistribution

Twenty-five BALB/c nude mice with U87 MG xenografts were randomly divided into 5 groups (5 mice in each) and were intravenously injected with ^{131}I -c(RGD)₂ dimer (0.74 MBq in 0.1 mL/mouse). Animals were sacrificed at 1, 3, 6, 14, and 24 h after injection. A 100 μL blood sample was obtained, and organs of interest were removed and weighed separately. Their radioactive counts were assessed using a \square -well counter (Beijing Nuclear Instrument Factory, Peking, China). The percent of injected dose per gram of tissue or per organ (% ID/g) was calculated as previously described^{22,23}.

Statistical Analysis

Values are presented as means \pm standard deviation. All statistical computations were performed using SPSS software (version 17.0).

Results**Radiolabeling of ^{131}I -c(RGD)₂**

The structure of the cRGD monomer with the lowest score was cyclic [-Cys-Arg-Gly-Asp-(D)Ser-Cys-]. To accelerate the clearance from the blood and non-target organs and minimize liver accumulation of the radiotracer, -Tyr-(D)Ser-Lys-(D)Ser-Ser- was designed as a bridge to link the two identical monomer sequences (Figure 1), as the (D)serine residues in the linker can modify the route of excretion and/or kidney retention²⁴. The tyrosine residue in the linker was designed to be

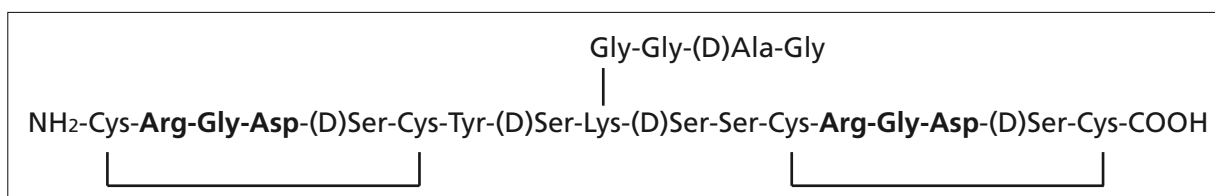


Figure 1. Amino acid sequence of the cyclic RGD dimer.

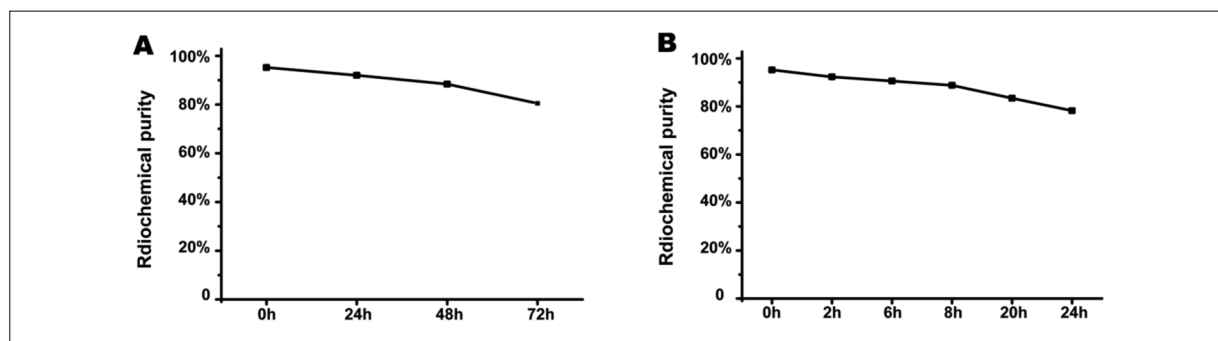


Figure 2. *In vitro* stability. Radiochemical purity of ^{131}I -c(RGD) $_2$ in 0.9% saline at 4°C (**A**) and in fresh human serum at 37°C (**B**).

labeled with ^{125}I and ^{131}I . In addition, -Gly-Gly-(D)Ala-Gly on the lysine residue was chosen as a chelating moiety to anchor $^{99\text{m}}\text{Tc}^{25}$. The relative molecular mass of the cRGD dimer was 2054.30, and the purity was over 95%.

The radiolabeling efficiency of the ^{131}I -c(RGD) $_2$ was $76.35\% \pm 2.33$, and radiochemical purities $> 95\%$ were obtained after purification. The product was stable for up to 6 h when stored in saline at 4°C (Figure 2A) or fresh human serum at 37°C (Figure 2B). The ^{131}I -c(RGD) $_2$ had a log p -value of -1.628 .

Cell Integrin Receptor-Binding Assay

To determine the binding affinity of ^{125}I -c(RGD) $_2$ to integrin $\alpha_5\beta_3$, a cell-binding assay was performed. Binding of the ^{125}I -c(RGD) $_2$ to integrin $\alpha_5\beta_3$ was obtained with non-radiolabeled c(RGD) $_2$ in a concentration-dependent manner. The K_d value was $(3.867 \pm 0.052) \times 10^{-9}$ M ($r = -0.976$, $p = 0.004$, Figure 3).

Imaging Study

Static SPECT scans were performed on mice with the U87 MG xenograft model. The U87 MG tumors were clearly visualized with a high contrast to the contralateral background at 3 and 6 h, and the uptake of the ^{131}I -c(RGD) $_2$ increased over time (Figure 4).

Biodistribution Study

The calculated %ID/g values of the U87 MG tumors and major tissues/organs are shown in Table I. At different times after administration of the ^{131}I -c(RGD) $_2$, the probe concentrated primarily in the kidneys and bladder, followed by the tumor. The blood data revealed that ^{131}I -c(RGD) $_2$ was characterized by rapid blood clearance, with 4.57 %ID/g remaining 1 h after administration

and 0.73 %ID/g remaining after 6 h. The specific uptake of the ^{131}I -c(RGD) $_2$ by tumor tissue increased after 1 h and remained at a relatively high level until 14 h post-injection. The calculated %ID/g was relatively high in the spleen, stomach, intestine, and liver at the 1-h time point but then decreased over time. As a result, the ratio of T/NT accumulation after the administration of ^{131}I -c(RGD) $_2$ increased as the time post-injection elapsed, particularly at the 24-h time point. The ratios of tumor-to-muscle (T/M) and tumor-to-blood (T/B) peaked at 4.29 and 5.00, respectively, at the 24-h time point.

Discussion

In this study, we successfully designed a novel cyclic RGD dimer that was efficiently labeled with ^{131}I using the CH-T method. It had high radiochemical purity, good stability, and high affinity.

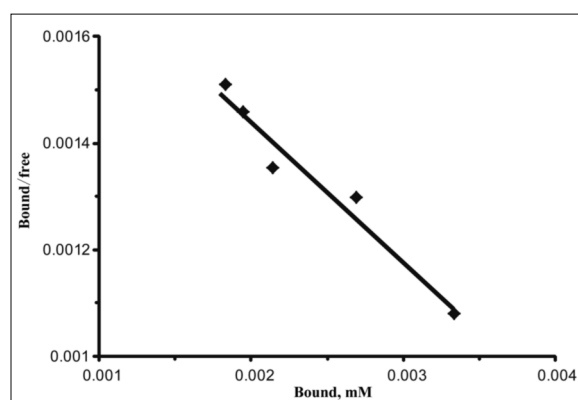


Figure 3. Scatchard plot of the binding test. Inhibition of the binding of ^{125}I -c(RGD) $_2$ to $\alpha_5\beta_3$ integrin was performed in U87 MG cells using non-radiolabeled c(RGD) $_2$.

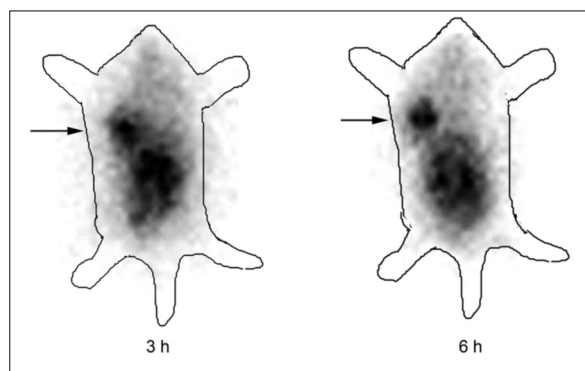


Figure 4. Planar imaging of tumor xenografts. Imaging of nude mice bearing U87 MG cells was conducted at 3 and 6 h following the administration of ^{131}I -c(RGD) $_2$. Tumors on the front right upper extremities are clearly shown.

We introduced (D)serine, a hydrophilic amino acid, to improve the hydrophilicity, which was validated by the octanol-water partition coefficient ($\log p$ -value = -1.628). Generally, compounds with a $\log p$ -value < 1 can be thought of as hydrophilic, while those with a $\log p$ -value > 4 are lipophilic. Therefore, the ^{131}I -c(RGD) $_2$ molecule had a hydrophilic characteristic that enabled it to redirect the excretion route toward the urinary system. This is particularly favorable for enhancing the clearance kinetics of the probe from non-cancerous organs, such as the liver, kidney, and lung¹⁴. The K_d value was $(3.867 \pm 0.052) \times 10^{-9}$ M, suggesting that the c(RGD) $_2$ molecule possessed a high integrin $\alpha_v\beta_3$ binding affinity and specificity.

The characteristics of the c(RGD) $_2$ molecule, including its binding affinity, specificity, and hydrophilicity were confirmed *in vivo* in U87 MG tumor-bearing mice by SPECT imaging and biodistribution experiments. Due to thyroid blockage, the concentration of the molecule in the thyroid glands was not evident during SPECT imaging. The tumors were clearly visualized at 3 and 6 h, and the uptake of ^{131}I -c(RGD) $_2$ increased over time. Substantial radioactivity accumulated in the abdomen due to rapid renal elimination. The biodistribution study was consistent with the imaging study. The tumor tissue showed higher accumulation of the peptide than other organs, except for the kidney. The initially rapid, high tumor concentration and much longer tumor retention could be attributed to the high integrin $\alpha_v\beta_3$ binding affinity of the tracers.

The *in vivo* imaging and biodistribution experiments revealed that the predominant clearance route of the ^{131}I -(RGD) $_2$ molecule was via the urinary system, and the uptake of radiotracer in the liver was low. The tumor/liver (T/L) ratio reached 4.92 at 24 h post-injection, providing further evidence for the high hydrophilic characteristics of the probe. Biodistribution data showed rapid blood clearance, with more than 68% of the peptide cleared at 3 h post-injection and 0.73 %ID/g remaining after 6 h. Due to the rapid clearance of the radiotracer, good T/B, T/L, and T/M ratios were achieved at 24 h after injection. The ratio of T/NT tissue is also a marker used to evaluate a potential tumor-imaging radiotracer. For clinical

Table I. Biodistribution data and tumor-to-normal tissue/organ ratio of ^{131}I -c(RGD) $_2$ in mice bearing U87 MG xenografts.

Tissue	1 h	3 h	6 h	14 h	24 h
Blood	4.57 \pm 1.81	1.43 \pm 0.24	0.73 \pm 0.10	0.70 \pm 0.18	0.15 \pm 0.04
Heart	1.04 \pm 0.20	0.61 \pm 0.07	0.42 \pm 0.06	0.41 \pm 0.15	0.09 \pm 0.03
Spleen	3.11 \pm 0.84	2.02 \pm 0.41	1.56 \pm 0.38	1.48 \pm 0.70	0.30 \pm 0.07
Liver	3.28 \pm 0.09	1.01 \pm 0.35	0.68 \pm 0.12	0.66 \pm 0.23	0.15 \pm 0.01
Lung	2.18 \pm 0.84	1.19 \pm 0.36	0.89 \pm 0.21	0.94 \pm 0.28	0.41 \pm 0.05
Kidney	12.49 \pm 2.83	7.55 \pm 0.80	6.67 \pm 0.68	2.16 \pm 0.75	0.62 \pm 0.04
Stomach	4.52 \pm 1.47	1.85 \pm 0.34	1.54 \pm 0.39	1.15 \pm 0.20	0.45 \pm 0.01
Small intestine	4.38 \pm 1.74	2.21 \pm 0.73	2.30 \pm 0.36	1.30 \pm 1.06	0.40 \pm 0.00
Bladder	6.53 \pm 2.94	3.93 \pm 1.18	2.74 \pm 1.15	3.91 \pm 1.30	0.48 \pm 0.11
Bone	0.83 \pm 0.71	1.16 \pm 0.32	0.95 \pm 0.27	0.67 \pm 0.13	0.25 \pm 0.06
Skeletal Muscle	4.38 \pm 0.41	1.52 \pm 0.71	0.74 \pm 0.37	0.77 \pm 0.33	0.17 \pm 0.01
Tumor	10.73 \pm 9.53	3.32 \pm 1.33	2.38 \pm 0.84	3.10 \pm 1.52	0.73 \pm 0.08
Tumor/Blood	2.08 \pm 1.32	2.40 \pm 1.06	3.20 \pm 0.76	4.32 \pm 1.08	5.01 \pm 0.75
Tumor/Muscle	2.38 \pm 1.94	2.46 \pm 1.25	3.40 \pm 0.87	4.05 \pm 0.80	4.29 \pm 0.77
Tumor/Liver	2.89 \pm 2.06	3.24 \pm 0.55	3.52 \pm 0.11	4.64 \pm 1.03	4.92 \pm 101
Tumor/Heart	4.72 \pm 3.95	5.43 \pm 1.91	5.57 \pm 1.15	7.85 \pm 2.50	8.46 \pm 1.85

Each value is expressed as an average plus/minus the standard deviation.

imaging, the T/NT ratio should reach 1.4-1.9²⁶. Therefore, the c(RGD)₂ molecule used in our study could be radionuclide-labeled for imaging.

cRGD [NH₂-Cys-Arg-Gly-Asp-Tyr-Cys-COOH (disulfide bridge: Cys¹-Cys⁶)] is a polypeptide that was reported by Liu et al²⁷. The accumulation of ¹³¹I-cRGD was only 1.39 %ID/g in melanoma xenograft tumors at 1 h after injection, which was much lower than the value of 10.73 %ID/g found in our study. The higher integrin $\alpha_v\beta_3$ binding affinity of ¹³¹I-c(RGD)₂ can be mainly explained by the dimerization of cRGD. Nevertheless, it should be noted that the integrin $\alpha_v\beta_3$ receptor exhibited a higher expression level in glioma xenografts than in melanoma xenografts, which also contributed to a greater accumulation of radiotracers in the tumor.

Liu et al²⁸ reported the polypeptide RGD-4CK, H₂N-Cys-Asp-Cys-Arg-Gly-Asp-Cys-Lys-Cys-COOH (disulfide bridge: Cys¹-Cys⁹, Cys³-Cys⁷). The liver uptake of ^{99m}Tc-RGD-4CK remained at 3.18% ID/g at 6 h after injection. Such substantial liver uptake and hepatobiliary excretion, which may result from its lipophilic characteristics, led to decreased image quality. Thus, it is not optimal for early liver cancer diagnosis. Our hydrophilic c(RGD)₂ molecule was designed to improve the excretion kinetics and to minimize liver uptake to reduce the accumulation of radioactivity in the upper abdominal area. Integrin $\alpha_v\beta_3$ is highly expressed in liver tumor cells and tumor vasculature²⁹. For this reason, it has the potential to improve the diagnostic rate and provide reliable evidence for liver cancer treatment. The c(RGD)₂ molecule used in our study was superior to RGD-4CK in this regard.

Conclusions

We successfully designed a new cyclic RGD dimer peptide, c(RGD)₂ with the assistance of a CADD system. The probe ¹³¹I-c(RGD)₂ presents suitable characteristics as an imaging agent for $\alpha_v\beta_3$ expression in tumor angiogenesis.

Acknowledgements

This research was supported by the Beijing Natural Science Foundation (7112129).

Conflict of Interest

The Authors declare that there are no conflicts of interest.

References

- 1) DESGROSELLIER JS, CHERESH DA. Integrins in cancer: biological implications and therapeutic opportunities. *Nat Rev Cancer* 2010; 10: 9-22.
- 2) LEE S, XIE J, CHEN X. Peptide-based probes for targeted molecular imaging. *Biochemistry* 2010; 49: 1364-1376.
- 3) DANHIER F, LE BRETON A, PRÉAT V. RGD-based strategies to target $\alpha_v\beta_3$ integrin in cancer therapy and diagnosis. *Mol Pharm* 2012; 9: 2961-2973.
- 4) TRAJKOVIC-ARSIC M, MOHAJERANI P, SARANTOPOULOS A, KALIDERIS E, STEIGER K, ESPOSITO I, MA X, THEMELIS G, BURTON N, MICHALSKI CW, KLEEFF J, STANGL S, BEER AJ, POHLE K, WESTER HJ, SCHMID RM, BRAREN R, NTZACHRISTOS V, SIVEKE JT. Multimodal molecular imaging of integrin $\alpha_v\beta_3$ for *in vivo* detection of pancreatic cancer. *J Nucl Med* 2014; 55: 446-451.
- 5) JIANG L, MIAO Z, LIU H, REN G, BAO A, CUTLER CS, SHI H, CHENG Z. ¹⁷⁷Lu-labeled RGD-BBN heterodimeric peptide for targeting prostate carcinoma. *Nucl Med Commun* 2013; 34: 909-914.
- 6) ALSIBAI W, HAHNENKAMP A, EISENBLÄTTER M, RIEMANN B, SCHÄFERS M, BREMER C, HAUFE G, HÖLTKE C. Fluorescent non-peptidic RGD mimetics with high selectivity for $\alpha_v\beta_3$ vs $\alpha_{IIb}\beta_3$ integrin receptor: novel probes for *in vivo* optical imaging. *J Med Chem* 2014; 57: 9971-9982.
- 7) TSIAPA I, LOUDOS G, FRAGOGEORGI EA, BOUZIOTIS P, PSIMADAS D, XANTHOPOULOS S, PARAVATOU-PETSOTAS M, PALAMARIS L, VARVARIGOU AD, KARNABATIDIS D, KAGADIS GC. Evaluation of $\alpha_v\beta_3$ -mediated tumor expression with a ^{99m}Tc-labeled ornithine-modified RGD derivative during glioblastoma growth *in vivo*. *Cancer Biother Radiopharm* 2014; 29: 444-450.
- 8) SEONG J, WANG N, WANG Y. Mechanotransduction at focal adhesions: from physiology to cancer development. *J Cell Mol Med* 2013; 17: 597-604.
- 9) ROBINSON SD, HODIVALA-DILKE KM. The role of β_3 -integrins in tumor angiogenesis: context is everything. *Curr Opin Cell Biol* 2011; 23: 630-637.
- 10) HAUBNER R, WESTER HJ, REUNING U, SENEKOWITSCH-SCHMIDTKE R, DIEFENBACH B, KESSLER H, STÖCKLIN G, SCHWAIGER M. Radiolabeled $\alpha_v\beta_3$ integrin antagonists: a new class of tracers for tumor targeting. *J Nucl Med* 1999; 40: 1061-1071.
- 11) MONTENEGRO CF, SALLA-PONTES CL, RIBEIRO JU, MACHADO AZ, RAMOS RF, FIGUEIREDO CC, MORANDI V, SELISTRE-DE-ARAÚJO HS. Blocking $\alpha_v\beta_3$ integrin by a recombinant RGD disintegrin impairs VEGF signaling in endothelial cells. *Biochimie* 2012; 94: 1812-1820.
- 12) SWITALA-JELEN K, DABROWSKA K, OPOLSKI A, LIPINSKA L, NOWACZYK M, GORSKI A. The biological functions of β_3 integrins. *Folia Biol (Praha)* 2004; 50: 143-152.
- 13) GAHMBERG CG, FAGERHOLM SC, NURMI SM, CHAVAKIS T, MARCHESAN S, GRÖNHOLM M. Regulation of inte-

- grin activity and signalling. *Biochim Biophys Acta* 2009; 1790: 431-444.
- 14) GAERTNER FC, KESSLER H, WESTER HJ, SCHWAIGER M, BEER AJ. Radiolabelled RGD peptides for imaging and therapy. *Eur J Nucl Med Mol Imaging* 2012; 39 (Suppl. 1): S126-S138.
 - 15) CAI H, CONTI PS. RGD-based PET tracers for imaging receptor integrin $\alpha_v\beta_3$ expression. *J Label Comp Radiopharm* 2013; 56: 264-279.
 - 16) LIU S. Radiolabeled cyclic RGD peptides as integrin $\alpha_v\beta_3$ -targeted radiotracers: maximizing binding affinity via bivalency. *Bioconjugate Chem* 2009; 20: 2199-2213.
 - 17) ZHOU Y, CHAKRABORTY S, LIU S. Radiolabeled cyclic RGD peptides as radiotracers for imaging tumors and thrombosis by SPECT. *Theranostics* 2011; 1: 58-82.
 - 18) SHI J, ZHOU Y, CHAKRABORTY S, KIM YS, JIA B, WANG F, LIU S. Evaluation of in-labeled cyclic RGD peptides: effects of peptide and linker multiplicity on their tumor uptake, excretion kinetics and metabolic stability. *Theranostics* 2011; 1: 322-340.
 - 19) CHAKRABORTY S, SHI J, KIM Y, ZHOU Y, JIA B, WANG F, LIU S. Evaluation of ^{111}In -labeled cyclic RGD peptides: tetrameric not tetravalent. *Bioconjugate Chem* 2010; 21: 969-978.
 - 20) PFAFF M, TANGEMANN K, MÜLLER B, GURRATH M, MÜLLER G, KESSLER H, TIMPL R, ENGEL J. Selective recognition of cyclic RGD peptides of NMR defined conformation by $\alpha_{\text{IIb}}\beta_3$, $\alpha_v\beta_3$, and $\alpha_5\beta_1$ integrins. *J Biol Chem* 1994; 269: 20233-20238.
 - 21) RUOSLAHTI E, PIERSCHBACHER MD. New perspectives in cell adhesion: RGD and integrins. *Science* 1987; 238: 491-497.
 - 22) SCHNEIDER DW, HEITNER T, ALICKE B, LIGHT DR, MCLEAN K, SATOZAWA N, PARRY G, YOO J, LEWIS JS, PARRY R. *In vivo* biodistribution, PET imaging, and tumor accumulation of ^{86}Y - and ^{111}In -anti-mindin/RG-1, engineered antibody fragments in LNCaP tumor-bearing nude mice. *J Nucl Med* 2009; 50: 435-443.
 - 23) KAISER CR, FLENNIKEN ML, GILLITZER E, HARMSSEN AL, HARMSSEN AG, JUTILA MA, DOUGLAS T, YOUNG MJ. Biodistribution studies of protein cage nanoparticles demonstrate broad tissue distribution and rapid clearance *in vivo*. *Int J Nanomed* 2007; 2: 715-733.
 - 24) ZHAO Q, YAN P, WANG RF, ZHANG CL, LI L, YIN L. A novel $^{99\text{m}}\text{Tc}$ -labeled molecular probe for tumor angiogenesis imaging in hepatoma xenografts model: a pilot study. *PLoS One* 2013; 8: e61043.
 - 25) LU X, ZHAO L, XUE T, ZHANG H. Technetium-99m-Arg-Arg-Leu(g2), a modified peptide probe targeted to neovascularization in molecular tumor imaging. *J BUON* 2013; 18: 1074-1081.
 - 26) BURAGGI C. Radioimmunodetection of cancer. *J Nucl Med Allied Sci* 1985; 29: 261-267.
 - 27) LIU HJ, WANG RF, ZHANG CL, YAN P, FU ZL, ZHANG XC, GUO FQ, LIU M, YU MM, DI LJ, DING L. Studies on distribution and imaging of ^{131}I -labelled RGD peptide in mice bearing tumors. *Chin J Med Imaging Technol* 2008; 11: 131-133.
 - 28) LIU B, FENG Y, ZHANG JY, LI HM, LI XD, JIA HL, LI ZY, FENG J. Imaging of bronchioloalveolar carcinoma in the mice with the $\alpha_v\beta_3$ integrin-targeted tracer $^{99\text{m}}\text{Tc}$ -RGD-4CK. *Transl Res* 2013; 162: 174-180.
 - 29) FOLKMAN J, PARRIS EE, FOLKMAN J. Tumor angiogenesis: therapeutic implications. *N Engl J Med* 1971; 285: 1182-1186.